

AFRL-IF-RS-TM-2001-1
In-House Technical Memorandum
July 2001



COMPLEX BAND-PASS FILTERS FOR ANALYTIC SIGNAL GENERATION AND THEIR APPLICATION

Andrew J. Noga

APPROVED FOR PUBLIC RELEASE; DISTRIBUTION UNLIMITED.

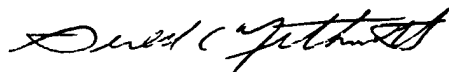
**AIR FORCE RESEARCH LABORATORY
INFORMATION DIRECTORATE
ROME RESEARCH SITE
ROME, NEW YORK**

20011109 074

This report has been reviewed by the Air Force Research Laboratory, Information Directorate, Public Affairs Office (IFOIPA) and is releasable to the National Technical Information Service (NTIS). At NTIS it will be releasable to the general public, including foreign nations.

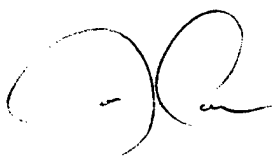
AFRL-IF-RS-TM-2001-1 has been reviewed and is approved for publication.

APPROVED:



GERALD C. NETHERCOTT
Chief, Multi-Sensor Exploitation Branch
Information & Intelligence Exploitation Division
Information Directorate

FOR THE DIRECTOR:



JOSEPH CAMERA
Chief, Information & Intelligence
Exploitation Division
Information Directorate

If your address has changed or if you wish to be removed from the Air Force Research Laboratory Rome Research Site mailing list, or if the addressee is no longer employed by your organization, please notify AFRL/IFEC, 32 Brooks Road, Rome, NY 13441-4114. This will assist us in maintaining a current mailing list.

Do not return copies of this report unless contractual obligations or notices on a specific document require that it be returned.

REPORT DOCUMENTATION PAGE

*Form Approved
OMB No. 0704-0188*

Public reporting burden for this collection of information is estimated to average 1 hour per response, including the time for reviewing instructions, searching existing data sources, gathering and maintaining the data needed, and completing and reviewing the collection of information. Send comments regarding this burden estimate or any other aspect of this collection of information, including suggestions for reducing this burden, to Washington Headquarters Services, Directorate for Information Operations and Reports, 1215 Jefferson Davis Highway, Suite 1204, Arlington, VA 22202-4302, and to the Office of Management and Budget, Paperwork Reduction Project (0704-0188), Washington, DC 20503.

1. AGENCY USE ONLY (Leave blank)		2. REPORT DATE JULY 2001	3. REPORT TYPE AND DATES COVERED In House Final, Feb 2000 - Feb 2001	
4. TITLE AND SUBTITLE COMPLEX BAND-PASS FILTERS FOR ANALYTIC SIGNAL GENERATION AND THEIR APPLICATION			5. FUNDING NUMBERS PE - 62702F PR - 459E TA - H0 WU- C1	
6. AUTHOR(S) Andrew J. Noga				
7. PERFORMING ORGANIZATION NAME(S) AND ADDRESS(ES) AFRL/IFEC 32 Brooks Road Rome, NY 13441-4114			8. PERFORMING ORGANIZATION REPORT NUMBER AFRL-IF-RS-TM-2001-1	
9. SPONSORING/MONITORING AGENCY NAME(S) AND ADDRESS(ES) AFRL/IFEC 32 Brooks Road Rome, NY 13441-4114			10. SPONSORING/MONITORING AGENCY REPORT NUMBER AFRL-IF-RS-TM-2001-1	
11. SUPPLEMENTARY NOTES Air Force Research Laboratory Project Engineer: Dr. Andrew J. Noga/IFEC/315-330-2270				
12a. DISTRIBUTION AVAILABILITY STATEMENT APPROVED FOR PUBLIC RELEASE; DISTRIBUTION UNLIMITED.			12b. DISTRIBUTION CODE	
13. ABSTRACT (Maximum 200 words) The generation of the pre-envelope and complex envelope of an arbitrary band-pass component of a digitized signal is presented. In particular, the complex band-pass filter method of analytic signal generation is generalized. Synchronization is also addressed and an example application of interference cancellation is given.				
14. SUBJECT TERMS Pre-envelope, complex envelope, analytic signal, synchronization, interference cancellation			15. NUMBER OF PAGES 32	
			16. PRICE CODE	
17. SECURITY CLASSIFICATION OF REPORT UNCLASSIFIED	18. SECURITY CLASSIFICATION OF THIS PAGE UNCLASSIFIED	19. SECURITY CLASSIFICATION OF ABSTRACT UNCLASSIFIED	20. LIMITATION OF ABSTRACT UL	

Table of Contents

1. Introduction	1
1.1 Review of Analytic Signal Representation	2
2. The Quadrature Down-converter	5
3. Complex Band-pass Filters	8
3.1 Complex Band-pass Filter Generation	9
3.2 Synchronization Considerations	12
3.3 Example Application: Interference Removal	16
4. Conclusions	21
5. References	22

List of Acronyms / Abbreviations

AM	Amplitude Modulation
AM-DSB-SC	Amplitude Modulation, Double Side-band Suppressed Carrier
ARMA	Auto-regressive Moving Average
CBPF	Complex Band-pass Filter
DAC	Digital-to-Analog Converter
DSP	Digital Signal Processing
FIR	Finite Impulse Response
FM	Frequency Modulation
I	In-phase
IIR	Infinite Impulse Response
LPF	Low-pass Filter
NBIC	Narrow-band Interference Canceller
Q	Quadrature-phase

1. Introduction

The concept of the Hilbert transform and the related application of analytic signal representation are well known and studied [1]. It is common practice in modern communications and radar signal processing systems, particularly those that are implemented digitally, to leverage the benefits of analytic representation. Among the more important benefits are the potential increase in spectral resolution for a given number of signal samples, and the ability to calculate instantaneous envelope and phase measurements from the resulting complex-valued signal. What is less well known is the fact that there are alternative methods of analytic signal generation that can alleviate problems associated with implementation issues such as real-time operation and signal synchronization. The goal of this report is to bring to light the implications of recent publication in this area, and to augment these results with recent AFRL in-house research results. In particular, recent published research introduces filter design considerations which can reduce computational complexity and simplify the design process [2]. In this report, this method is generalized for a wider range of filter designs and applications.

A quick review of the Hilbert transform and analytic signal representation is given in Section 1.1. For more detail, the reader is referred to [1]. Herein we are concerned with digital (i.e., numerical), uniformly sampled discrete-time sequences resulting from the proper acquisition of a corresponding analog signal of interest or from the computer generation of a signal of interest. In practice, one can certainly approximate Hilbert transforms and the analytic signal representation with analog waveforms. This method is described in Section 2. However, it can be shown that even with rather stringent specifications on in-phase (I) and quadrature (Q) channel balance (e.g., 0.1 dB amplitude and 1 degree phase imbalance), a modest amount (40 dB) of image distortion suppression will be achieved [3]. In many cases, the in-phase and quadrature channels are then digitized in preparation for further digital processing. In contrast, when generating the analytic signal computationally after digitization of the signal of interest [4, 5], the precision of the required calculations and the available processor resources (speed, memory, etc.) become the limiting factors on performance. This second method is described in Section 3, along with advancements to the method. Because of the recent advances in digital signal processing (DSP) hardware, this latter approach is often deemed more cost effective, particularly when image suppression greater than 40 dB

is required. Section 3 addresses often overlooked synchronization concerns, and provides a novel interference cancellation application. Section 4 provides a summary and conclusions.

1.1 Review of Analytic Signal Representation

A convenient method of explaining the concept of analytic signal representation relies on knowledge of some basic signals and systems theory. Although the term “analytic” has roots in the theory of complex variables, it will suffice here to say that this term refers to complex-valued continuous-time / continuous-amplitude signals, having specific continuity properties within the I and Q channel signal components. In this sense, it’s somewhat of a misnomer to refer to a digitized signal as being analytic, given the discrete nature of the signal. One can, however, generate good analog approximations to a true analytic signal by using a pair of digital-to-analog converters (DACs) and low-pass filters using the corresponding digital “analytic” signal. Therefore, for the remainder of this report we dismiss distinctions between the two, allowing the term “analytic signal” for the analog and digital cases. Herein we are ultimately interested in the digitized form of the analytic signal. However, continuous-time analytic signal generation is first described for contextual purposes.

The signal theory to be relied upon is now introduced. Of particular importance is Euler’s identity,

$$e^{j\alpha} = \cos(\alpha) + j \sin(\alpha). \tag{1-1}$$

This provides a mathematical framework for interpretation of pairs of separate real-valued signals, the real and imaginary components of Equation (1-1), as being a single but complex-valued signal. Here, α represents some phase signal that is a function of either continuous or discrete time, i.e., either $\alpha(t)$ or $\alpha(nT_s)$, and T_s is the sampling interval. Thus for an arbitrary index in time, n , the in-phase signal is $\cos(\alpha)$ and the quadrature signal is $\sin(\alpha)$. More generally, we can multiply both sides of Equation (1-1) by a real-valued envelope signal, $|\mathbf{a}|$, to account for changes in signal amplitude over time. As with α , $|\mathbf{a}|$ represents an envelope signal that is a function of either continuous or discrete time, i.e., either $|a(t)|$ or $|a(nT_s)|$.

From the modulation theorem it is known that any real band-pass signal, $s(t)$, can be represented as

$$s(t) = |a(t)| \cdot \cos(\alpha(t)), \quad (1-2)$$

where $|a(t)|$ is the envelope of $s(t)$, and $\alpha(t)$ is the phase. If we define the pre-envelope of $s(t)$ as

$$s_+(t) = |a(t)| \cdot e^{j\alpha(t)}, \quad (1-3)$$

from Equation (1-1) we have

$$s_+(t) = s(t) + j\hat{s}(t) = |a(t)| \cdot \{\cos(\alpha(t)) + j \sin(\alpha(t))\}. \quad (1-4)$$

The signal $\hat{s}(t) = |a(t)| \cdot \sin(\alpha(t))$ is the Hilbert transform of $s(t)$ ¹. This can be shown by using the mathematical definition of the Hilbert transform,

$$\hat{s}(t) = \frac{1}{\pi} \int_{-\infty}^{\infty} \frac{s(\tau)}{t - \tau} d\tau. \quad (1-5)$$

As can be seen, this time-domain representation has little intuitive appeal. The Hilbert transform has a much more intuitive meaning when viewed from a frequency-domain perspective as will be discussed below. However, the time-domain representation of Equation (1-5) implies that in order to obtain the exact transform, the integral is performed over all time. As with an exact Fourier transform, this is of course, impractical. In practice, the transform is approximated with filters that can actually be implemented. The trade-off areas in such approximations include filter time delays and non-ideal frequency responses that are typical with practical filters.

¹ The notation \hat{S} is being used here to signify the Hilbert transform of S , rather than the usual notation, \hat{S} ; the notation \hat{S} will be used to represent the estimate of some arbitrary signal, S .

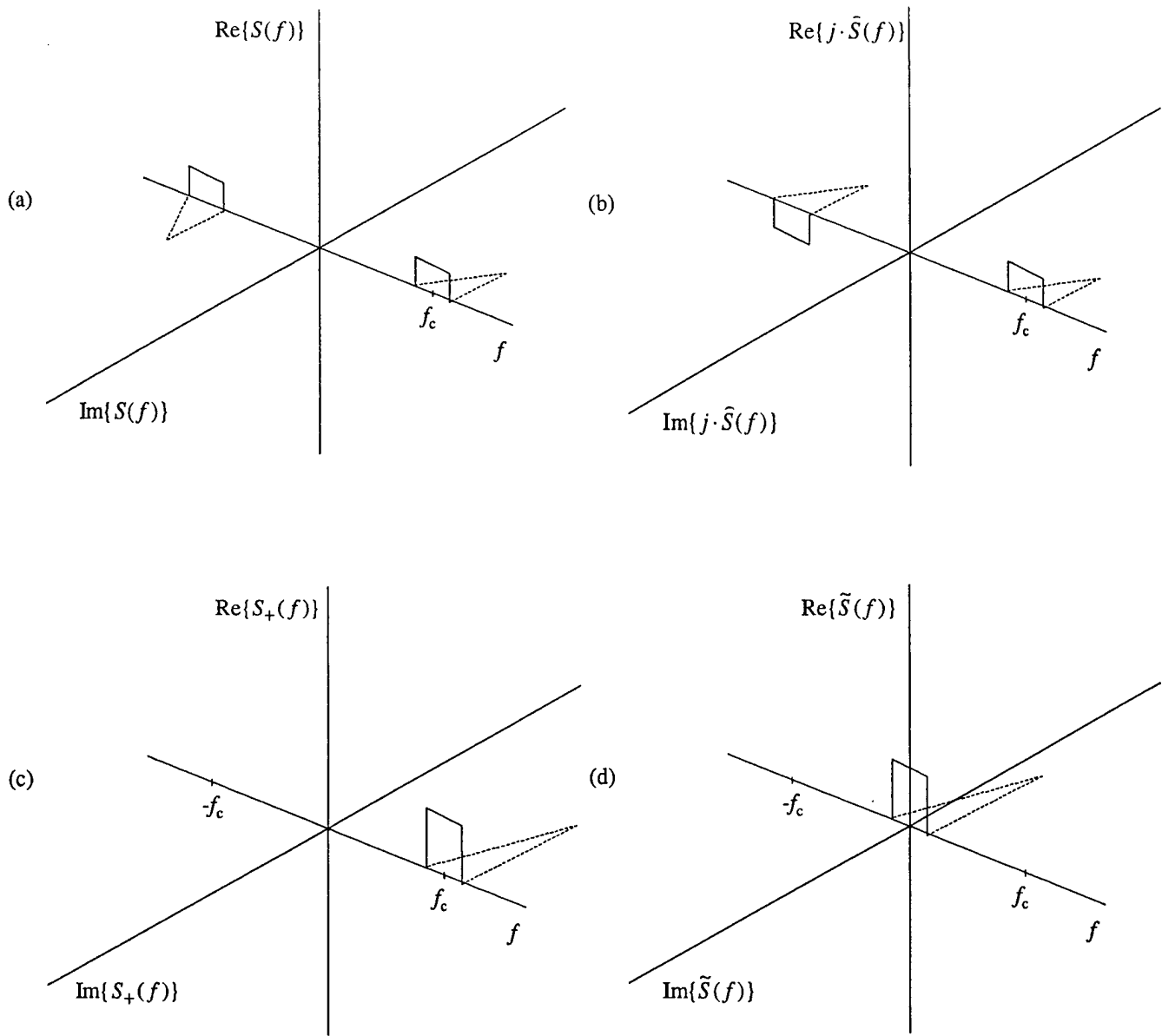


Figure 1-1. Representative band-pass signal spectra from the Hilbert transform method of complex envelope generation; (a) the spectrum of the original real signal, $s(t)$, (b) the spectrum of j times the Hilbert transform, $\hat{s}(t)$, of $s(t)$, (c) the spectrum of the pre-envelope, $s_+(t) = s(t) + j\hat{s}(t)$, and (d) the spectrum of the complex envelope, $\tilde{s}(t)$, of $s(t)$.

Figures 1-1 (a) through 1-1 (d) help to describe the Hilbert transform process. In Figure 1-1 (a) is presented a representative spectrum of an arbitrary band-pass signal, $s(t)$. Note that the Fourier transform of a real signal is conjugate symmetric as depicted in the figure. Fourier transformation of

the signal of Equation (1-5) can be shown to result in a 90 degree phase shift in the frequency components of $s(t)$. Shown in Figure 1-1 (b) is the spectrum of the product $j \cdot \hat{s}(t)$. Multiplication of the Hilbert transform by the complex constant, j , and adding this to the original signal, results in the pre-envelope, $s_+(t)$, as described by Equation (1-4).

Note that the resulting signal spectrum has no energy below $f = 0$. The utility of this process is apparent through inspection of Equation (1-4). With the I signal, $s(t)$, and the Q signal, $\hat{s}(t)$, one can calculate the envelope as $\sqrt{s^2(t) + \hat{s}^2(t)}$, and the instantaneous phase as $\alpha_i(t) = \text{Arc tan}[\hat{s}(t)/s(t)]$. Alternatively, the pre-envelope can be down-converted in frequency to 0, by multiplying by $e^{-j2\pi f_c t}$, where f_c is the center frequency of the pre-envelope. This results in the complex envelope,

$$\tilde{s}(t) = s_+(t) \cdot e^{-j2\pi f_c t} \quad (1-6)$$

Representing the pre-envelope phase component as $\alpha(t) = 2\pi f_c t + \phi(t) + \theta$, the phase of the complex envelope is $\phi(t) + \theta$, where θ is some constant. The spectrum of the complex envelope is depicted in Figure 1-1 (d). In practice, approximations to the complex envelope are more commonly used, rather than pre-envelope approximations. As described in Section 3, however, this leads to unnecessary additional computations when working with digitized signals. Practical methods of approximating the complex envelope can now be presented.

2. The Quadrature Down-converter

Also referred to in the literature as the quadrature mixer or quadrature demodulator, the quadrature down-converter represents a practical solution to the problem of complex envelope approximation. The basic structure of the quadrature down-converter is shown in Figure 2-1 (a). It consists of a signal splitter, and a pair of mixer and low-pass filter combinations. The intent of the device is to accomplish the elimination of the negative frequency components seen in Figure 1-1 (a) and frequency down-conversion consistent with the desired spectrum of Figure 1-1 (d). This is achieved by performing the down-conversion first, then low-pass filtering with the appropriate

(identical) low-pass filter in each channel. In the ideal case, if the splitters, mixers, and low-pass filters were ideal processes with perfect gain and phase responses, then a signal proportional to the complex envelope is obtained by interpreting the device output as $i(t) + jq(t)$. (The proportionality constant factor of 2 is easily accounted for.) The ideal result will be a pure downward translation in frequency and rejection by the low-pass filters of signal content that occurs in the vicinity of $2f_c$. This signal content is expected, is due to the mixing process itself, and is normally easily removed by the filters. However, in practice, distortions arise in the form of attenuated and phase-delayed images of the desired spectral components. In effect, the down-conversion process contains an undesired up-converted signal component that is also located at 0 Hz, creating the additive image distortion signal.

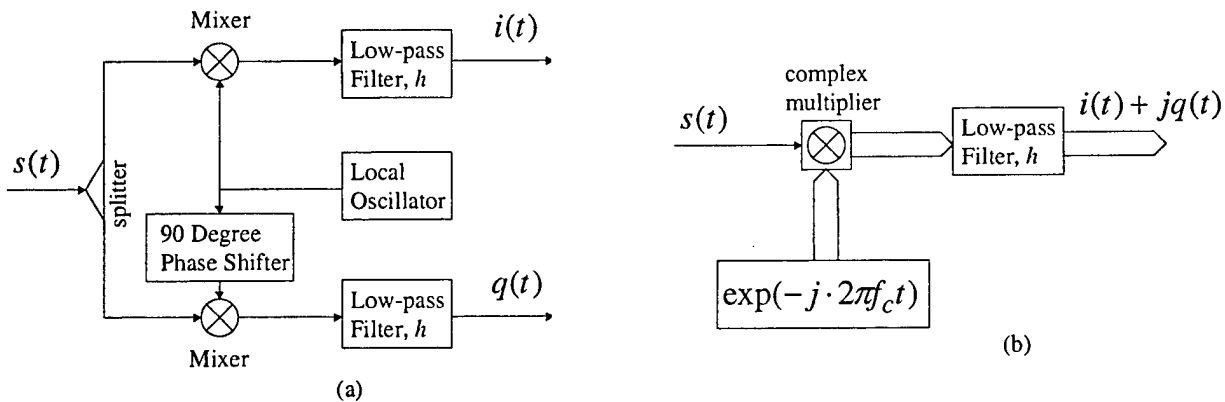


Figure 2-1. The quadrature down-converter method of complex envelope generation; (a) the physical representation, (b) the mathematical representation.

The mathematical representation of the quadrature down-conversion process is shown in Figure 2-1 (b). Comparing the physical and mathematical representations, the local oscillator and phase shifter processes are approximations to the signal $\exp(-j2\pi f_c t)$. The splitter and mixer processes attempt to achieve the same result as complex-valued multiplication of this locally generated signal by the real input signal, $s(t)$. The pair of real-valued identical low-pass filters accomplishes the rejection of out-of-band frequency components, consistent with the rules of complex arithmetic. These rules imply the need for a pair of identical filters, one operating on the in-phase channel and the other operating on the quadrature channel. In contrast, the mathematical system

requires a single real low-pass filter operating on the complex-valued signal output from the complex multiplier.

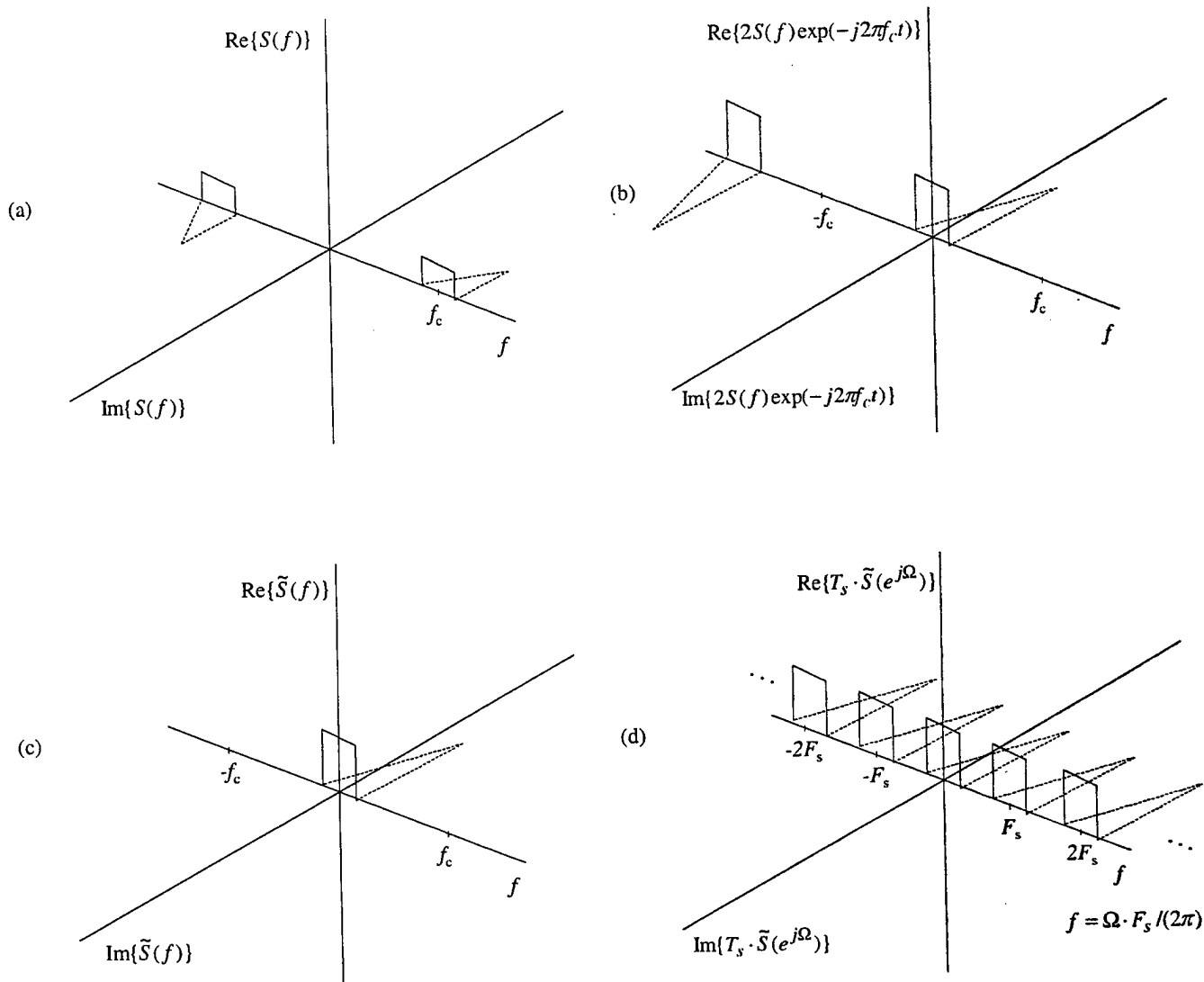


Figure 2-2. Representative band-pass signal spectra from the ideal quadrature down-converter method of complex envelope generation; (a) the spectrum of the original real signal, $s(t)$, (b) the spectrum of the down-converted signal, $2s(t)\exp(-j2\pi f_c t)$, (c) the spectrum of the complex envelope, $\tilde{s}(t)$, resulting from ideal low-pass filtering and (d) the spectrum of the sampled complex envelope, $\tilde{s}(nT_s)$, at the sampling interval $T_s = 1/F_s$.

Once the in-phase and quadrature signals have been generated by the quadrature down-converter, a pair of identical, synchronized analog-to-digital converters are used to acquire the analytic signal. Shown in Figure 2-2 are representative spectra for the various steps in the ideal quadrature down-converter, including the sampling process. Although there are practical issues such as gain and phase imbalance between the channels, filter delays and local oscillator synchronization, it can be seen that the quadrature down-converter represents a viable method of complex envelope generation. In fact, methods of characterizing and compensating for channel imbalance have been studied [6 - 9]. A commonly used alternative is to first digitize the signal of interest and then implement a numerical (i.e., digital) quadrature down-converter. This leads to the less known concept of complex band-pass filters.

3. Complex Band-pass Filters

The generalization of a method of generating the discrete-time pre-envelope and complex envelope signals from a properly sampled band-pass signal is now presented. Advancements are made to the work of Reilly, Frazer and Boashash [2], where the special case which employs complex FIR (Finite Impulse Response) band-pass filtering has been treated. The generalization presented herein, includes the extension to the IIR (Infinite Impulse Response) case, and the extension to the case where synchronization to a reference is of concern. These extensions allow for further practical application of the complex band-pass filtering process.

With the work of [2], the concept of complex (band-pass) filtering for generation of the discrete analytic signal has been introduced. (Related observations regarding the relationship of symmetric half-band low-pass filters, Hilbert transformers, and analytic signal generation, have been previously made by Jackson [10].) As the name implies, complex band-pass filtering involves the generation of a pre-envelope signal, achieved via linear convolution of the real input signal with a filter represented by an appropriate set of complex-valued filter coefficients. As will be shown, these coefficients are easily derived from the design of a real low-pass filter, of appropriate frequency response characteristics. This real low-pass filter will be referred to herein as the low-pass filter prototype.

Any common method of generating the coefficients of this low-pass filter prototype may be used, including the popular Parks-McClellan algorithm, and window-based designs [11]. The same

design considerations used in generating the low-pass filter of the half-band filter method [10] or the low-pass filter pair of the commonly employed quadrature down-conversion method [12] of complex envelope generation are used in designing the low-pass prototype. (For example, if the cut-off frequency of the prototype filter is $B/2$ Hz, then the bandwidth of the resulting complex band-pass filter will be B Hz.) Once the pre-envelope is generated via complex band-pass filtering, the modulation theorem indicates that one can easily rotate the pre-envelope down in frequency to a center frequency of 0, resulting in the complex envelope. Thus it can be shown that the quadrature down-conversion and complex band-pass filtering processes can produce equivalent results.

As in [2], this equivalence is leveraged herein and allows for the formulation of the complex band-pass filter coefficients. However, rather than being limited to the FIR case, the results given in Section 3.1 also apply to the more general IIR case. Interest in IIR solutions is evidenced in [11, 13, 14]. One reason for this interest is that it is often the case that FIR filters meeting the same specifications are of substantially larger order.

In spite of the simplicity of the complex band-pass filter, practical issues arise when attempting to use either this or any equivalent method of analytic signal generation. In particular, situations often arise in synchronization applications, where filter time delays must be taken into account in order to alleviate phase offsets. In subsequent sections it is shown how to avoid such problems. An example of the complex band-pass filter method of pre-envelope generation is given, emphasizing the IIR case and synchronization problem.

3.1 Complex Band-Pass Filter Generation

Based on the relationship of the quadrature down-conversion method of complex envelope generation and the complex band-pass filter method of pre-envelope generation, the coefficients of the complex band-pass filter can be derived. Consider the low-pass prototype filter impulse response, $h_{lp}(nT_s)$, and its z-transform, $H_{lp}(z)$. For the ARMA (Auto-Regressive Moving-Average) filter model, which includes both the FIR and IIR cases, $H_{lp}(z)$ is of the form

$$H_{lp}(z) = \frac{\sum_{k=0}^M b_k \cdot z^{-k}}{\sum_{k=0}^N a_k \cdot z^{-k}} \quad (3-1)$$

The impulse response, $h_{lp}(nT_s)$, is determined by the $2+M+N$ real coefficients b_k , $k=0,1,2,\dots,M$ and a_k , $k=0,1,2,\dots,N$. (Here, T_s is the sample interval in seconds, and the corresponding sample rate is $F_s = 1/T_s$ samples per second.) The filter response $H_{lp}(z)$ corresponds to the response of either of the identical real low-pass filters used in the quadrature down-conversion process.

The z-transform of a filter $h(nT_s)$ is by definition

$$H(z) = \sum_{n=-\infty}^{\infty} h(nT_s) \cdot z^{-n} . \quad (3-2)$$

Therefore when the low-pass filter prototype is appropriately modulated, the resulting complex sequence,

$$h_{lp}(nT_s) e^{+j2\pi f_1 n T_s} ,$$

has the z-transform

$$h_{lp}(nT_s) e^{+j2\pi f_1 n T_s} \stackrel{z}{\leftrightarrow} H_+(z) = H_{lp}(z \cdot e^{-j2\pi f_1 T_s}) . \quad (3-3)$$

Thus for filters of the form presented in Equation (3-1) we have

$$\begin{aligned} H_+(z) &= \frac{\sum_{k=0}^M b_k \cdot \{z \cdot e^{-j2\pi f_1 T_s}\}^{-k}}{\sum_{k=0}^N a_k \cdot \{z \cdot e^{-j2\pi f_1 T_s}\}^{-k}} \\ &= \frac{\sum_{k=0}^M \{b_k \cdot e^{+j2\pi f_1 k T_s}\} \cdot z^{-k}}{\sum_{k=0}^N \{a_k \cdot e^{+j2\pi f_1 k T_s}\} z^{-k}} . \end{aligned} \quad (3-4)$$

Equations (3-3) and (3-4) imply that any filter with the response as indicated in Equation (3-1) can be circularly rotated in frequency by the amount f_i Hz, by multiplying the finite length real coefficient sequences a_k and b_k by the complex exponential sequence,

$$e^{+j\Omega_i k} = e^{+j2\pi f_i k T_s} \quad (3-5)$$

The resulting complex-valued coefficients are those of the desired complex band-pass filter, $h_+(nT_s)$, the response of which is given in Equation (3-4). The complex band-pass filter numerator coefficients become

$$d_k = b_k \cdot e^{+j\Omega_i k}, \quad k = 0, 1, 2, \dots, M, \quad (3-6a)$$

the denominator coefficients become

$$c_k = a_k \cdot e^{+j\Omega_i k}, \quad k = 0, 1, 2, \dots, N. \quad (3-6b)$$

Thus we can transform a properly designed prototype low-pass filter of the quadrature down-converter with low-pass bandwidth $B/2$, into a complex band-pass filter with band-pass bandwidth B and centered at $+f_i$ Hz. Subsequently, we can linearly convolve the input sequence with this complex filter. The result of this convolution, a positive pre-envelope, can then be circularly rotated down in frequency to yield the corresponding complex envelope signal if so desired, for e.g. FM demodulation [15]. This is consistent with the results of [2], with the important exception that the method of complex filter coefficient generation of Equations (3-6a) and (3-6b) includes not only the FIR case, but also the more general IIR case. *Note also that we have not limited ourselves to the case where the entire positive frequency range is of interest, as defined by the pre-envelope of the input sequence. Rather, the pre-envelope of any band-pass constituent of the input signal can be obtained.*

3.2 Synchronization Considerations

The rather simple looking results of Equations (3-6a) and (3-6b), are not without associated subtleties. To better appreciate these subtleties, we now consider the application of the complex band-pass filter method, to problems involving synchronization. Without loss of generality, we consider the two-component case where a narrow-band constituent, $s_1(nT_s)$, of the input signal, $s(nT_s) = s_1(nT_s) + s_2(nT_s)$, is of interest. (The term “narrow-band” is being used relative to the sample rate, $F_s / 2$.) It is assumed that the pre-envelope of $s_1(nT_s)$ must be extracted, without loss of phase reference to $s_2(nT_s)$. (A continuous-time example of such a synchronization problem, is that of commercial FM stereo reception. Subsequent to FM demodulation, a pilot tone at 19 KHz is used to synchronously demodulate an AM-DSB-SC constituent at 38 KHz, which contains the L-R audio component [16].) The approximate center frequency of $s_1(nT_s)$ is taken to be $\Omega_1 = 2\pi f_1 T_s$ radians per second. As it turns out, the choice of the rotation sequences of Equations (3-6a) and (3-6b), has an effect on the ability to achieve synchronization. In the application of Equations (3-6a) and (3-6b), the rotation sequences, $e^{+j\Omega_1 k}$, used in the products shown were each conveniently assigned an index, k , corresponding to the indices of the filter coefficients.

This index assignment will often suffice, but more generally, the indices must be carefully selected to achieve a desired phase relationship, and need not be integer valued in the exponent. Taking this into account, we rewrite Equations (3-6a) and (3-6b) as

$$d_{]x-y[} = b_{]x-y[} \cdot e^{+j\Omega_1 x}, \quad x = y, y+1, y+2, \dots, y+M, \quad (3-7a)$$

$$c_{]x-y[} = a_{]x-y[} \cdot e^{+j\Omega_1(x+\Delta)}, \quad x = y, y+1, y+2, \dots, y+N. \quad (3-7b)$$

Here, we are using the notation $]x-y[$, for the nearest integer value of the quantity $x-y$. In order to determine the proper values for the index, y , and for the offset, Δ , we need to consider the processing involved in the corresponding quadrature down-conversion method of pre-envelope generation when applied to the synchronization problem. The block diagram of such a system for generating the pre-envelope of $s_1(nT_s)$, is shown in Figure 3-1. This system for generating the pre-envelope, $s_{1+}(nT_s)$, of the constituent $s_1(nT_s)$, has been carefully designed to take into account the effective time delay,

$n_o T_s$, of the low-pass filter, $h_p(nT_s)$. By pre-determining and using the sample delay, n_o , in the system of Figure 3-1, a pre-envelope is generated that remains synchronized to the delayed input signal constituent, $s_1([n-n_o]T_s)$. This further implies that the phase relationship with the delayed constituent, $s_2([n-n_o]T_s)$, has also been maintained and can therefore be readily used to process $s_2([n-n_o]T_s)$.

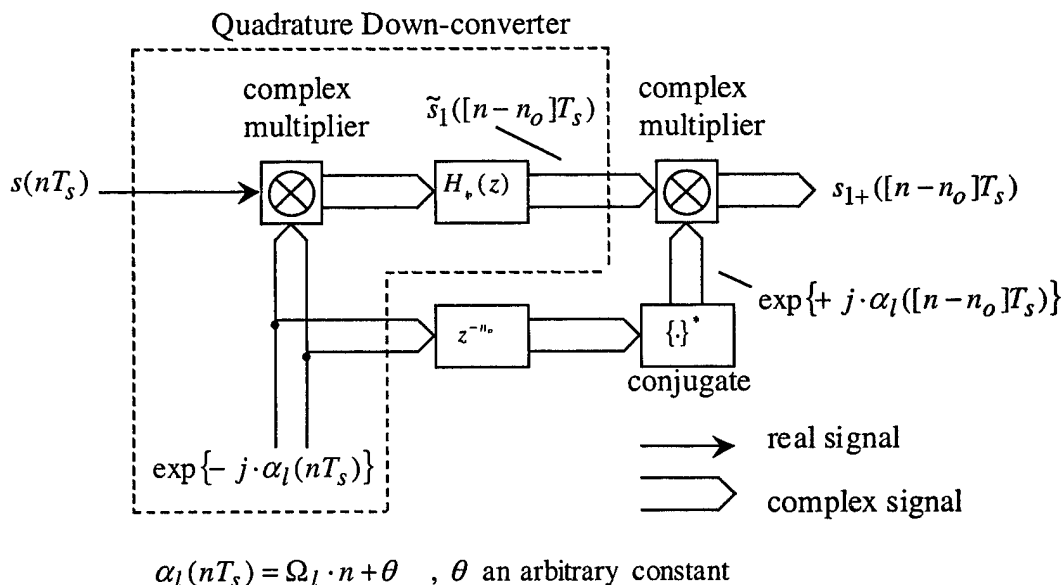


Figure 3-1. Pre-envelope generation using the quadrature down-converter, with phase relationships of signal constituents maintained.

Analyzing the response of the system of Figure 3-1, we can determine the offset, Δ , that will yield the equivalent complex band-pass filter, $h_+(nT_s)$, when using Equations (3-7a) and (3-7b). It can be shown that the equivalent complex band-pass filter is obtained when $\Delta = n_o$. Also, the numerator filter coefficients can be made conjugate symmetric by setting $y = -M/2$. This can lead to a lower number of computations when implementing the filter, if the low-pass prototype is a symmetric FIR filter.

As an example, results from a MATLAB-based simulation are presented. In this simulation, $s_1(nT_s)$ and $s_2(nT_s)$ are both unity amplitude sinusoids of frequencies 0.23 and 0.69 Hz respectively. Likewise, the phase angle of $s_2(nT_s)$ is three times that of $s_1(nT_s)$. These signals are summed to form the input, $s(nT_s) = s_1(nT_s) + s_2(nT_s)$, to a complex band-pass filter which is used to

generate the pre-envelope, $s_{1+}([n-n_o]T_s)$, of the constituent $s_1(nT_s)$. It is then graphically demonstrated that the phase relationship with the delayed constituent, $s_2([n-n_o]T_s)$, has been maintained. This is accomplished by tripling the phase and frequency of the pre-envelope, $s_{1+}([n-n_o]T_s)$, and using the real part of this result as the estimate of $s_2([n-n_o]T_s)$. Samples of both the true constituent, $s_2([n-n_o]T_s)$, and the estimate are shown in Figure 3-2. (The starting sample has been chosen well after filter transients have subsided.)

The prototype low-pass filter is a 16th order digital Butterworth filter with a specified cut-off of .09765 Hz relative to $F_s = 2$ samples per second, resulting from the MATLABTM "butter.m" routine [17]. In this example, the pre-envelope of a band-pass constituent located at $f_i = 0.23$ Hz is of interest. This filter has been intentionally designed such that n_o is approximately integer valued, and in this case $n_o \cong 33$ samples. As seen in Figure 3-2 (a), when we arbitrarily set $\Delta = 0$, the complex band-pass filter resulting from Eqs. (3-7a) and (3-7b) imparts an undesired phase on the estimate of $s_2([n-n_o]T_s)$. In contrast to this, when we set $\Delta = n_o \cong 33$, synchronization between the estimated and true signals is achieved as shown in Figure 3-2 (b).

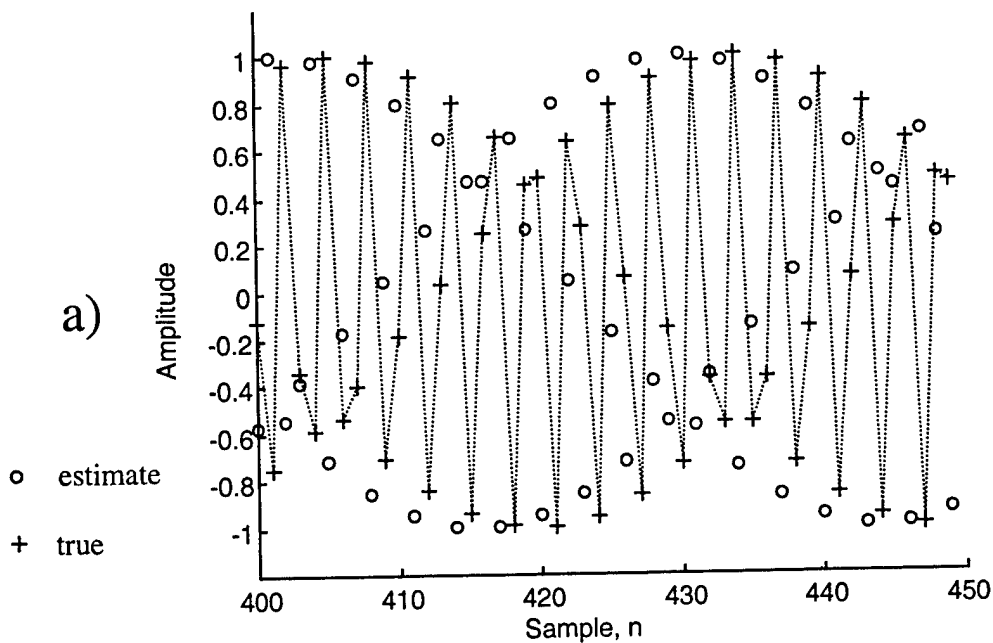


Figure 3-2. (a) Segments of the estimated and true sequences of the constituent $s_2([n-33]T_s)$, with $\Delta = 0$ and $n_o \cong 33$; synchronization is not achieved.

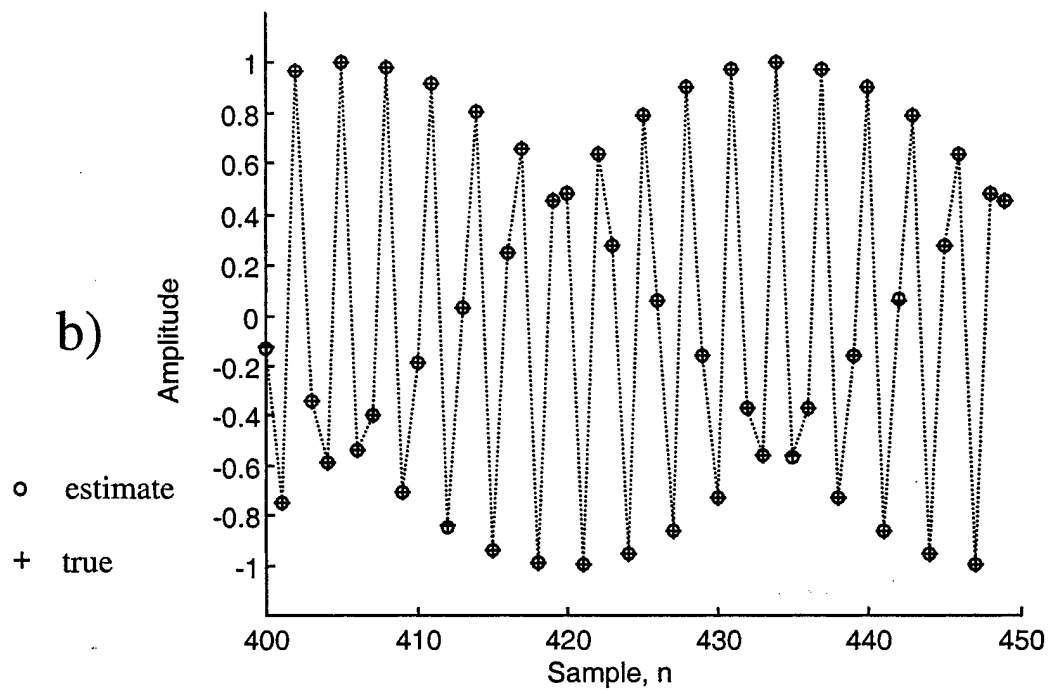


Figure 3-2. (b) Segments of the estimated and true sequences of the constituent $s_2([n - 33]T_s)$, with $\Delta = n_o \cong 33$; synchronization is achieved.

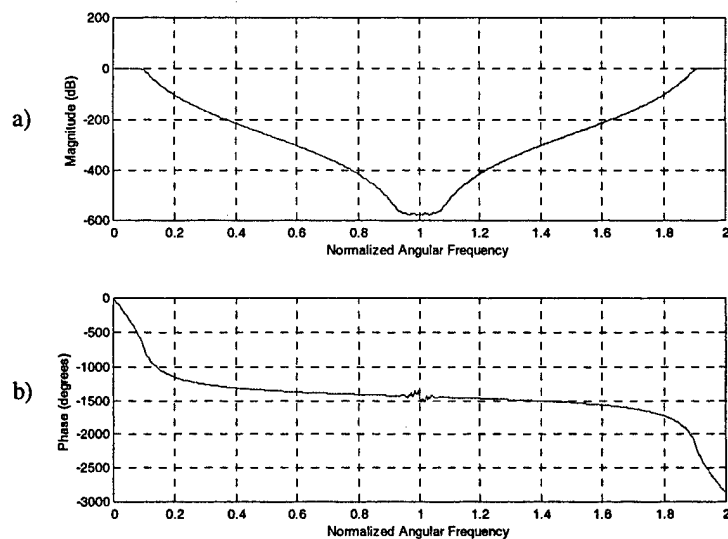


Figure 3-3. Example prototype low-pass filter and resulting complex band-pass filter responses; (a) low-pass filter magnitude response, (b) low-pass filter phase response,

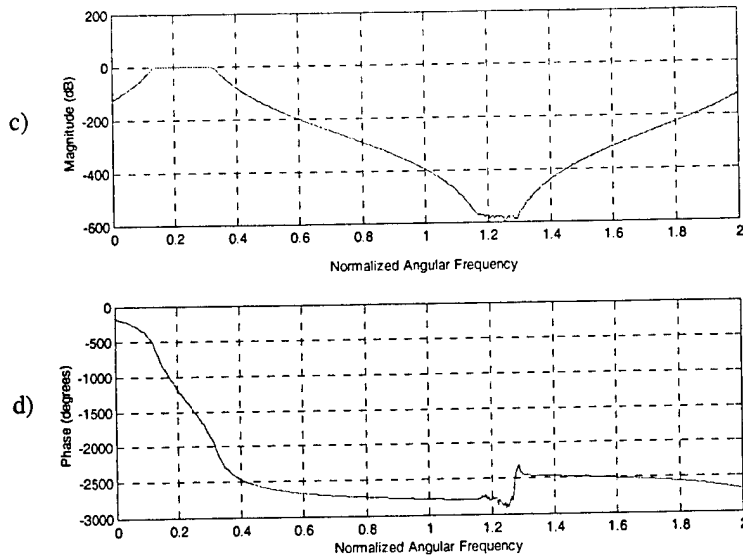


Figure 3-3. (c) complex band-pass filter magnitude response, (d) complex band-pass filter phase response.

Figure 3-3 shows the responses of the prototype Butterworth low-pass filter and the corresponding complex band-pass filter. Note that the response has been rotated in frequency to 0.23 Hz.

3.3 Example Application: Interference Removal

The additional example of maintaining signal synchronization for the purpose of interference cancellation provides further insight into potential applications. The cancellation technique to be presented in this section has been applied in [18] to enhance speaker identification in the presence of narrow-band interference. For convenience, a description of the method is also given in this report.

Narrow-band interference can be removed via notch filtering prior to processes such as demodulation. For removal of pure tonal interference, the notch filter approach can be very effective. One can design a notch filter with a small bandwidth such that only a small amount of the desired signal is attenuated when the tone is removed. However, in practical communication settings, interfering signals can have non-infinitesimal bandwidths. A more sophisticated technique is required to handle such cases.

The interference cancellation technique/device proposed by the author and presented herein,

will be referred to as the narrow-band interference canceller (NBIC). The basic NBIC device is shown in Figure 3-4. Although it is somewhat more complicated relative to the notch filter method, it is also observed to be more robust in scenarios where the interfering signal is angle-modulated. The input to the device,

$$X(nT_s) = s(nT_s) + D(nT_s), \quad (3-8)$$

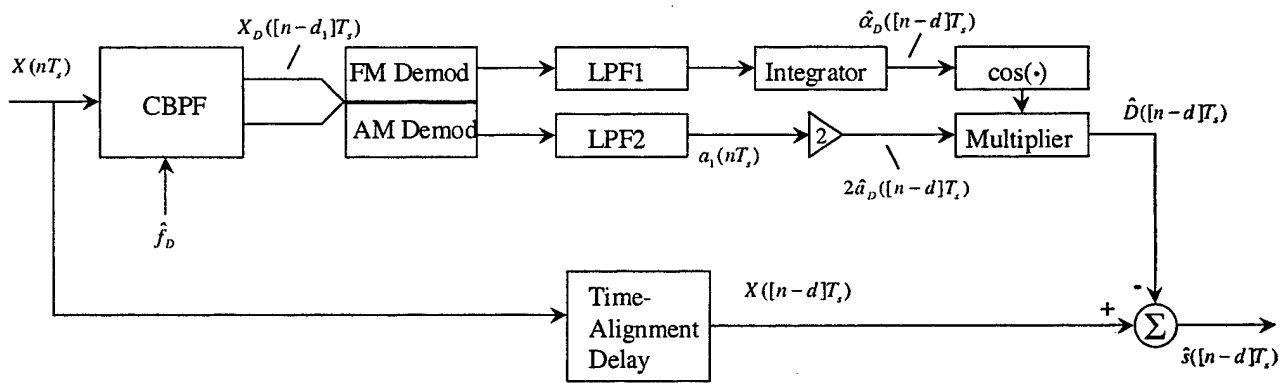


Figure 3-4. A narrow-band interference canceller.

consists of the sum of a desired signal $s(nT_s)$, and an interfering distortion signal, $D(nT_s)$, and is sampled at $F_s = 1/T_s$ samples per second. For the given configuration of the NBIC, it is assumed that $D(nT_s)$ is much narrower in bandwidth than $s(nT_s)$, and can be modeled as

$$D(nT_s) = 2|a_D(nT_s)| \cdot \cos(\alpha_D(nT_s)), \quad (3-9)$$

where $\alpha_D(nT_s) = 2\pi f_D nT_s + \phi_D(nT_s) + \theta_D$. Here, $2|a_D(nT_s)|$ is the slowly varying envelope and f_D is the center frequency of $D(nT_s)$. The angle modulation which is present consists of $\phi_D(nT_s)$ and the constant (dc) phase term, θ_D . Referring to the figure, the function of the complex band-pass filter (CBPF) is to pass, with unity gain, frequencies in a narrow band about the center frequency estimate,

\hat{f}_D , and to reject all other frequencies (both positive and negative). In an initialization process, the set of complex valued coefficients for the CBPF are generated based on this center frequency estimate. To create the CBPF, Equations (3-7) (a) and (b) are applied, with $\Delta = d_1$, where d_1 is the time delay (in samples) imparted by the low-pass filter prototype. The output of the CBPF is an estimate of the pre-envelope of $D(nT_s)$, and is represented as

$$X_D(n_1T_s) = |A_D(n_1T_s)| \cdot \exp(j \cdot \{\alpha_D(n_1T_s) + e(n_1T_s)\}), \quad (3-10)$$

where $n_1 = n - d_1$. The envelope of the distortion estimate is $|A_D(nT_s)| = |a_D(nT_s) + E(nT_s)|$. The errors, $E(nT_s)$ and $e(nT_s)$ are an additive envelope error and an additive phase error, respectively. These errors are the combined result of the component of $s(nT_s)$ which passes through the CBPF, and the errors arising from the convolution of $D(nT_s)$ with the CBPF. These effects are minimized by proper selection of the bandwidth of the CBPF. Nominally, this bandwidth is set equal to the bandwidth of $D(nT_s)$. $X_D(nT_s)$ can be represented in rectangular notation as

$$X_D(nT_s) = X_{Di}(nT_s) + jX_{Dq}(nT_s), \quad (3-11)$$

where

$$X_{Di}(nT_s) = |A_D(nT_s)| \cdot \cos(\alpha_D(nT_s) + e(nT_s)), \quad (3-12)$$

and

$$X_{Dq}(nT_s) = |A_D(nT_s)| \cdot \sin(\alpha_D(nT_s) + e(nT_s)). \quad (3-13)$$

This representation facilitates the demodulation processes, using the pair of real signals, $X_{Di}(nT_s)$, and $X_{Dq}(nT_s)$.

Before proceeding with the descriptions of the remaining processes, it is noted that overall, the complex band-pass filter, CBPF, and the low-pass filters, LPF1 and LPF2, will impart a delay relative to the input signal. This fact is taken into account in the NBIC, by designing these filters such that a total delay of d samples is imparted, relative to the input. LPF1 and LPF2 are designed to impart equal delays since the FM Demod and Integrator together impart a zero sample delay, as does the AM Demod. Thus the delay of CBPF is d_1 samples, and the delays of LPF1 and LPF2 are both $(d - d_1)$ samples.

The AM demodulation (AM Demod) and low-pass filtering (LPF2) processes, are readily accomplished, and result in

$$\begin{aligned} a_1(nT_s) &= \left[\sqrt{X_{Di}^2([n - d_1]T_s) + X_{Dq}^2([n - d_1]T_s)} \right]_{LPF2} \\ &= \left[A_D([n - d_1]T_s) \right]_{LPF2}. \end{aligned} \quad (3-14)$$

The notation $[\cdot]_{LPF2}$ represents the low-pass filtering process depicted in the figure as LPF2. From (3-14) and the definition of $A_D(nT_s)$, we have that

$$\hat{a}_d([n - d]T_s) = \left[a_d([n - d_1]T_s) + E([n - d_1]T_s) \right]_{LPF2}. \quad (3-15)$$

To be consistent with (3-9), we note the need for a gain of 2 as shown in Figure 3-4, for restoration of the envelope. The function of LPF2 is to reject, to the extent possible, the envelope error component, $E(nT_s)$.

The FM demodulation (FM Demod) process is implemented as a first-backward-difference operation on the recovered phase sequence

$$\alpha_{2\pi}(nT_s) = \text{Arc tan} \left[\frac{X_{Dq}(nT_s)}{X_{Di}(nT_s)} \right]. \quad (3-16)$$

This difference is calculated in a modulo- 2π fashion, often referred to as phase unwrapping. (More correctly, this is referred to as phase-difference quadrant determination.) The Arctan in (3-16) is the four-quadrant arctangent of the ratio of quadrature and in-phase components, X_{Dq} , and X_{Di} . In the absence of phase cycle-slips, the low-pass filtering (LPF1) and Integrator processes result in the distortion phase estimate

$$\hat{\alpha}_D([n-d]T_s) = [\alpha_D([n-d]T_s) + e([n-d]T_s)]_{LPF1}. \quad (3-17)$$

The function of LPF1 is to reject, to the extent possible, the phase error component, $e(nT_s)$. The Integrator process, in the case where a backward-difference FM demodulator is used, is simply an accumulator, with a specific initial condition. This initial condition is set equal to the initial phase, $\alpha_{2\pi}(-T_s)$, used in the FM demodulation process. (For simplicity the initial phase is set to zero.) Note that for practical purposes, the integration process can also be calculated modulo- 2π , preventing large accumulation results. Thus, the function of the Integrator is to invert the FM demodulation process. The FM demodulation process itself, has facilitated the use of LPF1.

With the envelope and phase estimates of $D(nT_s)$ available, the $\cos(\cdot)$ and Multiplier processes are used to generate the estimate

$$\hat{D}([n-d]T_s) = 2\hat{a}_D([n-d]T_s) \cdot \cos(\hat{\alpha}_D([n-d]T_s)). \quad (3-18)$$

Finally, as shown, after properly aligning the input with the distortion estimate, the distortion estimate is subtracted from the input signal, resulting in an estimate of the desired signal,

$$\hat{s}([n-d]T_s) = X([n-d]T_s) - \hat{D}([n-d]T_s). \quad (3-19)$$

Thus the Time-Alignment Delay imparts a delay of d samples on the input, allowing for a synchronous subtraction process.

4. Conclusions

Generation of the discrete-time pre-envelope or complex envelope signals from a sampled band-pass signal, is a fundamental pre-processing step in modern signal processing systems, with applications including sonar, radar, audio and communication processing systems. The complex band-pass filter method presented herein provides the system designer with a simple means of analytic signal generation which leverages existing real low-pass filter design tools. Extensions are made to the cited previous work in which the special case of the FIR complex band-pass filter was presented. These extensions include the more general IIR complex band-pass filter, and applications where synchronization is of concern. An example has been presented which both employs an IIR complex band-pass filter and demonstrates how to maintain phase synchronization. The concepts provided in the example were then built upon to provide a more sophisticated example application of interference cancellation. The results presented allow for further understanding and practical application of the complex band-pass filtering process.

As presented in [4], the digital quadrature down-converter represents an enhancement to the traditional analog process. In particular, with appropriately designed filters and proper arithmetic precision, the image distortion present in analog implementations is kept within acceptable limits in the digital implementation. With the work of [2], advantage is taken of the equivalence of FIR complex band-pass filters and digital quadrature down-converters with FIR low-pass filters. This leads to the elimination of the need for complex sequence generation and multiplication at every sampling instant. Instead, the FIR filters themselves are pre-rotated in frequency, forming the complex band-pass filter used for subsequent convolution. Designers of the digital quadrature down-converter have cleverly avoided complicated sequence generation by judicious choice of the sample rate and center frequency of the signal of interest. However, this limits the flexibility of the analytic signal generation process. (It should be noted that rotation of the center frequency of the pre-envelope signal to 0 Hz is unnecessary; in particular, as with envelope demodulation, angle demodulation does not require the complex envelope [15].)

Both the FIR complex band-pass filter process of [2] and the digital quadrature down-converter of [4] address only the case where the entire positive frequency band is of interest. In the most general case, any band-pass signal in the Nyquist range may be of interest. The extensions presented in this report allow for the arbitrary selection of center frequency and bandwidth. More

recently, poly-phase filter banks (see e.g., [19]) are becoming popular for the selection of band-pass signals that are less than full Nyquist bandwidth. However, the standard applications of such poly-phase methods are for inputs with equally spaced frequency channels. This and the often-used additional constraint of perfect reconstruction, limits the choices of filter responses available to the designer. In general, where no such channelization is required, the complex band-pass filter represents an attractive alternative when signal fidelity, bandwidth and frequency selection flexibility are desired.

5. References

- [1] Haykin, S., *Communication Systems*, 4th Ed., John Wiley & Sons, New York, 2000.
- [2] Reilly, A., Frazer, G., Boashash, B., "Analytic Signal Generation - Tips and Traps," *IEEE Transactions on Signal Processing*, Vol. 42, pp. 3241-3245, November 1994.
- [3] Monzingo, R. A., "Evaluation of Image Response Signal Power Resulting from I-Q Channel Imbalance," *IEEE Transactions on Aerospace and Electronic Systems*, Vol. AES-23, No. 2, March 1987.
- [4] Mitchell, R. L., "Creating Complex Signal Samples from a Band-limited Real Signal," *IEEE Transactions on Aerospace and Electronic Systems*, Vol. 25, No. 3, January 1989.
- [5] Ho, K. C., Chan, Y. T., Inkol, R., "A Digital Quadrature Demodulation System," *IEEE Transactions on Aerospace and Electronic Systems*, Vol. 32, No. 4, October 1996.
- [6] Churchill, F. E., Ogar, G. W., Thompson, B. J., "The Correction of I and Q Errors in a Coherent Processor," *IEEE Transactions on Aerospace and Electronic Systems*, Vol. AES-17, No. 1, January 1981.
- [7] Kafadar, K., "Statistical Calibration of a Vector Demodulator," *Hewlett-Packard Journal*, June 1988.
- [8] Loper, R. K., "A Tri-Phase Conversion Receiver," *Military Communications Conference, MILCOM '90*, IEEE, 1990.
- [9] Pun, K., Franca, J. E., Azeredo-Leme, C., "Wideband Digital Correction of I and Q Mismatch in Quadrature Radio Receivers," *IEEE International Symposium on Circuits and Systems*, May 28-31, 2000.
- [10] Jackson, L. B., "On the Relationship Between Digital Hilbert Transformers and Certain Low-Pass Filters," *IEEE Transactions on Acoustics Speech and Signal Processing*, Vol. 23, pp. 381-383, August 1975.

- [11] Oppenheim, A. V., Schaffer, R. W., *Discrete-Time Signal Processing*, Prentice Hall, 1989.
- [12] Urkowitz, H., *Signal Theory and Random Processes*, Artech House, 1983.
- [13] Schüssler, H. W., Weith, J., "On the Design of Recursive Hilbert-Transformers," *Proceedings of the IEEE International Conference on Acoustics Speech and Signal Processing*, pp. 876-879, April 1987.
- [14] Alkhairy, A., "Design of Optimal IIR Filters with Arbitrary Magnitude," *IEEE Transactions on Circuits and Systems-II: Analog and Digital Signal Processing*, Vol. 42, No. 9, September 1995.
- [15] Noga, A. J., Sarkar, T. K., "A Discrete-Time Method of Demodulating Large Deviation FM Signals," *IEEE Transactions on Communications*, Vol. 47, No. 8, August 1999.
- [16] Stremmler, F. G., *Introduction to Communication Systems*, 2nd Ed., Addison-Wesley, 1982.
- [17] Little, J., Shure, L., *Signal Processing Toolbox User's Guide for Use with MATLABTM*, Natick, MA, The Mathworks, Inc., 1988.
- [18] Wenndt, S. J., Noga, A. J., "Narrow-band Interference Cancellation for Enhanced Speaker Identification," *Proceedings of the 1999 IEEE Workshop on Applications of Signal Processing to Audio and Acoustics*, October 1999.
- [19] Schuller, G. D. T., Karp, T., "Modulated Filter Banks with Arbitrary System Delay: Efficient Implementations and the Time-Varying Case," *IEEE Transactions on Signal Processing*, Vol. 48, No. 3, March 2000.

***MISSION
OF
AFRL/INFORMATION DIRECTORATE (IF)***

The advancement and application of Information Systems Science and Technology to meet Air Force unique requirements for Information Dominance and its transition to aerospace systems to meet Air Force needs.